Bilecik Şeyh Edebali Üniversitesi Fen Bilimleri Dergisi
Bilecik Şeyh Edebali University Journal of Science
e-ISSN: 2458-7575 (https://dergipark.org.tr/tr/pub/bseufbd)

Araştırma Makalesi – Research Article

Geliş Tarihi / Received: 03/02/2025

Kabul Tarihi / Accepted: 06/08/2025

Yayın Tarihi / Published: 30/11/2025

In-silico Drug Evaluation by Molecular Docking and ADME Studies, DFT Calculations of 2-(4-Chlorobenzyl)-6-(4-methoxyphenyl)imidazo [2,1-b][1,3,4]thiadiazole

2-(4-Klorobenzil)-6-(4-metoksifenil)imidazo[2,1-b][1,3,4]tiadiazol'un DFT Hesaplamaları, ADME Çalışmaları ve Moleküler Doking ile in-silico İlaç Değerlendirmesi

Kenan Gören[1*], Mehmet Bağlan[2], Veysel Tahiroğlu[3], Ümit Yıldıko[4]

[1*]Kafkas University/ Institute of Science/ Faculty of Arts and Sciences/ Department of Organic Chemistry/ Kars, Türkiye/ kenangoren49@gmail.com/ https://orcid.org/0000-0001-5068-1762

[2]Kafkas University/ Institute of Science/ Faculty of Arts and Sciences/ Department of Organic Chemistry/ Kars, Türkiye/ mehmetbaglan36@gmail.com/ https://orcid.org/0000-0002-7089-7111

[3]Şırnak University/ Institute of Health Sciences/ Faculty of Health Sciences/ Department of Nursing/ Şırnak, Türkiye/ veysel0793@hotmail.com/ https://orcid.org/0000-0003-3516-5561

[4]Kafkas University/ Faculty of Engineering and Architecture/ Department of Bioengineering/ Kars, Türkiye/ yildiko1@gmail.com/ https://orcid.org/0000-0001-8627-9038

Ethical Statement: It is declared that scientific and ethical principles were followed during the preparation of this study and that all studies used are stated in the bibliography.

Artificial Intelligence Ethical Statement: The author declares that artificial intelligence was not utilized at any stage of the preparation process of this article and accepts full responsibility in this regard.

Conflicts of Interest: The author(s) has no conflict of interest to declare.

Grant Support: The author(s) acknowledge that they received no external funding to support this research.

Etik Beyan: Bu çalışmanın hazırlanma sürecinde bilimsel ve etik ilkelere uyulduğu ve yararlanılan tüm çalışmaların kaynakçada belirtildiği beyan olunur.

Yapay Zeka Etik Beyanı: Yazar bu makalenin hazırlanma sürecinin hiçbir aşamasında yapay zekadan faydalanılmadığını; bu konuda tüm sorumluluğun kendisine(kendilerine) ait olduğunu beyan etmektedir.

Çıkar Çatışması: Çıkar çatışması beyan edilmemiştir.

Finansman: Bu araştırmayı desteklemek için dış fon kullanılmamıştır.

In-silico Drug Evaluation by Molecular Docking and ADME Studies, DFT Calculations of 2-(4-Chlorobenzyl)-6-(4-methoxyphenyl)imidazo [2,1-b][1,3,4]thiadiazole

ABSTRACT

The discovery of the imidazo[2,1-b][1,3,4]thiadiazole heterocycle was seen in the 1950s. The pharmacological potential of imidazo[2,1-b][1,3,4]thiadiazole derivatives as antibacterial, antifungal, anticonvulsant, anticancer, analgesic, anti-inflammatory, diuretic, and anesthetic has been extensively studied. The present investigation is to examine the 2-(4-Chlorobenzyl)-6-(4-methoxyphenyl)imidazo[2,1-b][1,3,4]thiadiazole (CMT) compound theoretically with the Gaussian 09 software program. The mentioned compound's theoretical calculations were done on using the popular density functional theory (DFT) theories B3LYP, MPW1PW91 methods, the 6-311G(d,p) basis set. The highest occupied molecular orbital (HOMO), lowest unoccupied molecular orbital LUMO, natural bonding orbital NBO, nonlinear optical (NLO), molecular electrostatic potential (MEP), and Mulliken charges of the optimized structure were calculated theoretically with the same basis set and different methods, and the obtained values were compared with each other. Additionally, in silico studies were conducted to estimate the absorption, distribution, metabolism, excretion and toxicity (ADME) profiles of CMT compound to evaluate it as a drug. Based on the ADME study, we believe that the compound will have good potential drug-like character. Finally, 3PP0 and 1M17 enzymes were downloaded from PDB (Protein Data Bank) and the potential of CMT compound on breast cancer was calculated in silico by molecular docking analysis. According to the docking analysis outcomes, the docking score of CMT compound was obtained as -10.20 and -7.50 kcal/mol, respectively. In the docking analysis, it was shown that the theoretical data on breast cancer were well correlated with the observed values.

Keywords-Molecular Docking, DFT, NBO, MEP, ADME

Highlights

- This study theoretically investigates the structural, electronic, and biological properties of 2-(4-chlorobenzyl)-6-(4-methoxyphenyl)imidazo[2,1-b][1,3,4]thiadiazole (CMT) as a potential anticancer drug candidate.
- The compound was optimized using DFT methods (B3LYP and MPW1PW91) with the 6-311G(d,p) basis set, and key parameters such as HOMO–LUMO energies, NBO, NLO, MEP, and Mulliken charges were calculated.
- Comparative analysis of theoretical results showed strong agreement between the two DFT approaches, confirming the molecule's stability and charge distribution characteristics.
- In silico ADME evaluation revealed that CMT possesses favorable drug-like properties and acceptable pharmacokinetic behavior.
- Molecular docking studies against 3PP0 and 1M17 breast cancer enzymes yielded significant binding affinities (–10.20 and –7.20 kcal/mol, respectively), supporting its potential as an effective anticancer agent.

2-(4-Klorobenzil)-6-(4-metoksifenil)imidazo[2,1-b][1,3,4]tiadiazol'un DFT Hesaplamaları, ADME Çalışmaları ve Moleküler Doking ile in-silico ilaç değerlendirmesi

ÖZ

İmidazo[2,1-b][1,3,4]tiadiazol heterosiklünün keşfi 1950'lerde görüldü. İmidazo[2,1-b][1,3,4]tiadiazol türevlerinin antibakteriyel, antifungal, antikonvülsan, analjezik, antikanser, antiinflamatuar, diüretik ve anestezik olarak farmakolojik potansiyeli kapsamlı bir şekilde incelenmiştir. Mevcut araştırma, 2-(4-Klorobenzil)-6-(4-metoksifenil)imidazo[2,1-b][1,3,4]tiadiazol (CMT) bileşiğini Gaussian 09 yazılım programı ile teorik olarak incelemektir. Bahsedilen bileşiğin teorik hesaplamaları, popüler yoğunluk fonksiyonel teorisi (DFT) teorileri

B3LYP, MPW1PW91 metotlar 6-311G(d,p) temel set kullanılarak yapılmıştır. Optimize edilmiş yapının en yüksek dolu moleküler orbitali (HOMO), en düşük boş moleküler orbitali LUMO, doğal bağ orbitali NBO, doğrusal olmayan optik (NLO), moleküler elektrostatik potansiyeli (MEP), ve Mulliken yükleri aynı temel set ve farklı metotlar teorik olarak hesaplandı ve elde edilen değerler birbirleriyle kıyaslandı. Ek olarak, CMT bileşiğinin bir ilaç olarak değerlendirilmesi için emilim, dağılım, metabolizma, atılım ve toksisite (ADME) profillerini tahmin etmek için in silico çalışmalar yürütülmüştür. ADME çalışmasına dayanarak, bileşiğin iyi bir potansiyel ilaç benzeri karaktere sahip olacağına inanıyoruz. Son olarak, 3PP0 ve 1M17 enzimleri PDB'den (Protein Veri Bankası) indirildi ve CMT bileşiğinin meme kanseri üzerindeki potansiyeli moleküler doking analizi ile in silico olarak hesaplandı. Doking analizi sonucununa göre, CMT bileşiğinin doking skoru sırasıyla -10.20 ve -7.20 kcal/mol olarak elde edildi. Doking analizinde, meme kanseri hakkındaki teorik verilerin gözlenen değerlerle iyi bir şekilde ilişkili olduğu gösterildi.

Anahtar Kelimeler- Moleküler Doking, MEP, DFT, NBO, ADME

Öne Çıkanlar

- Bu çalışma, potansiyel bir antikanser ilaç adayı olarak 2-(4-klorobenzil)-6-(4-metoksifenil)imidazo[2,1-b][1,3,4]tiadiazolün (CMT) yapısal, elektronik ve biyolojik özelliklerini teorik olarak incelemektedir.
- Bileşik, 6-311G(d,p) temel setiyle DFT yöntemleri (B3LYP ve MPW1PW91) kullanılarak optimize edilmiş ve HOMO–LUMO enerjileri, NBO, NLO, MEP ve Mulliken yükleri gibi temel parametreler hesaplanmıştır.
- Teorik sonuçların karşılaştırmalı analizi, iki DFT yaklaşımı arasında güçlü bir uyum olduğunu göstererek molekülün kararlılığını ve yük dağılımı özelliklerini doğrulamıştır.
- Silico ADME değerlendirmesi, CMT'nin olumlu ilaç benzeri özelliklere ve kabul edilebilir farmakokinetik davranışa sahip olduğunu ortaya koymuştur.
- 3PP0 ve 1M17 meme kanseri enzimlerine karşı yapılan moleküler yerleştirme çalışmaları, önemli bağlanma afinitesi (sırasıyla -10,20 ve -7,20 kcal/mol) sağlayarak, etkili bir kanser karşıtı ajan olarak potansiyelini desteklemektedir.

I. INTRODUCTION

In medicinal chemistry research, the imidazo[2,1-b][1,3,4] thiadiazole moiety is a significant family of heterocyclic molecules. Because of their diverse biological effects, imidazo[2,1-b][1,3,4]thiadiazole derivatives have been outlined in several publications in the literature [1]. These compounds have antibacterial, anti-inflammatory, anticonvulsant, antituberculosis, anticancer, and antihyperlipidemic properties, according to the most recent and pertinent research [2]. Indeed, the 1,3,4-thiadiazole nucleus is present in a number of commercially available medications, including sulfamethizole, cefazedone, cefazolin, and ceftezol (used as antibacterial medications) and acetazolamide and methazolamide (carbonic anhydrase inhibitors for the treatment of glaucoma). However, because of its significant biological effects and synthetic uses, benzimidazole and its derivatives are becoming increasingly essential in medicinal chemistry Investigation [3]. A fundamental structural component of several significant medications, including albendazole, mebendazole, thiabendazole, rabeprazole, and others, is benzoimidazole. Benzimidazole derivatives have demonstrated encouraging antituberculosis efficacy in a number of recent investigations.

Computer-aided quantum chemical calculations are calculations that combine quantum mechanics and computer science. These types of calculations are used to understand and predict the behavior of chemical systems. Quantum chemistry is a field that aims to understand chemical reactions at the atomic and molecular level, and these calculations can provide much more precise and accurate results [4]. Computer-aided quantum chemical calculations increase the speed and accuracy of scientific research, allowing us to make more accurate and effective designs at the atomic and molecular level. It continues to revolutionize many fields such as chemistry, biology, materials science, and engineering. Gaussian is a widely used software package for chemical calculations [5].

DFT is a theory used in quantum chemistry to study solids and molecules' the electronic structure. DFT is used to calculate the energy and characteristics of a system based on the electron density in the system. While traditional quantum chemistry calculations use the wave functions of electrons to determine the energy of a system, DFT performs these calculations on the electron density [6]. This approach is more computationally efficient, yet can still provide fairly accurate results. Computational efficiency allows DFT to analyze very large systems because it requires much less computational power than traditional wave function-based methods. It can be used

on a variety of systems, including molecules, solids, and liquids. DFT is considered an approach that provides accurate results, especially in predicting energies and structures [7].

The condition known as cancer occurs when cells proliferate and expand out of control, harming the tissues around them. These unchecked cells have the ability to spread (metastasize) to the body's healthy tissues and organs. Because the body contains a wide variety of cells, all of which have the potential to develop into cancer, there are several forms of cancer [8]. The kind, stage, and overall health of the patient all influence the symptoms and treatment options for cancer. Breast cancer, lung cancer, prostate cancer, colon cancer, and skin cancer (melanoma) are among the common forms of cancer. One kind of cancer that results from aberrant cell development and proliferation in the breast tissue is breast cancer. Although it is a type of cancer that can be treated with early diagnosis and treatment, it can become more challenging at certain stages. Breast cancer is usually seen in women, but it can also occur in men rarely [9].

In this study, compound 2-(4-Chlorobenzyl)-6-(4-methoxyphenyl)imidazo[2,1-b][1,3,4]thiadiazole (CMT) [10] was theoretically investigated with B3LYP, MPW1PW91 methods and 6-311G(d,p) basis set. Then, molecular docking (with 4DRH and 3PP0 enzymes) and ADME analysis were performed to evaluate the potential of CMT molecule on breast cancer and as a potential drug candidate.

II. METHODS

The CMT molecule was drawn from the ChemDraw program. The drawn molecule was optimized with the Gaussian09 program [11]. The most stable conformations were computed utilizing the B3LYP, MPW1PW91 methods and 6-311G(d,p) basis set in the DFT technique. Enzymes required for docking analysis were downloaded from PDB (Protein Data Bank) [12]. Schrödinger Maestro (version 11.8) was utilized for the CMT molecule's docking analysis [13]. Discovery Studio program was utilized to visualize the docking analysis outcomes [14]. An online tool such as SwissADME (http://www.swissadme.ch/index.php) was utilized to ADME analysis of the CMT molecule.

III. RESULTS

A. Structure Details and Analysis

Gaussian theoretical calculations are a powerful tool widely used in chemistry and physics to analyze molecular structures and energies. Geometry optimization is the calculations made for the structure of a molecule to reach the lowest energy state [15, 16]. This process is done to optimize the geometry (arrangement of atoms) of the molecule and to obtain a certain structure. Gaussian software is a software that performs such theoretical calculations. Geometry optimization is the calculations made to change a molecule's the structure parameters (bond angles, bond lengths) [17]. The aim is to determine the most suitable (stable) configuration of the system in terms of energy by minimizing the energy function of a molecule. Using the DFT method and polarizing functions added to eliminate the polarization effect, the geometry of this molecule in the gas phase was drawn utilizing the GaussView 6.0.16 program. Using the Gaussian09 program [11], the bond lengths, bond angles and planar bond angles of the molecule were calculated utilizing B3LYP, MPW1PW91 methods and the 6-311G(d,p) basis set, and these calculated data have been shown in Table 1. By the time we examine the data calculated in Table 1, we observed that the bond angles and lengths calculated utilizing the same basis set and different methods are compatible with each other by taking values close to each other. We observed that the C-C bond lengths are in the range of 1.37394 (Å), -1.42544 (Å) and the values in the literature are close. When we examine the literature, we observed that the bond lengths of the carbon atom with other atoms are close to each other [18]. We observed that the bond angles and planar bond angles calculated with different methods are compatible by taking values close to each other. The CMT molecule's optimized geometry utilizing the B3LYP 6-311G(d,p) method and basis set has been given in Figure 1. When the bond lengths obtained in the theoretical calculations for the selected 2-(4-Chlorobenzyl)-6-(4-methoxyphenyl)imidazo[2,1-b][1,3,4]thiadiazole (CMT) molecule were examined, the thiadiazole ring C–S bond; values for the CMT molecule: C1–S2 = 1.85994Å, C3–S2 = 1.72981Å (B3LYP), S1–C (thiadiazole) bond was seen as 1.756–1.772Å (S1–C1 =1.756Å, S1–C4 =1.736Å) in similar compounds in the literature [19]. For N–C and N–N bonds in the imidazothiadiazole ring; values for the CMT molecule were seen as: C3–N4 = 1.34976Å, C3–N6 = 1.35949Å, Another study: C–N bond=1.304Å, N–N=1.366Å, C–N=1.304Å. Values for the CMT molecule were seen as; C–N bonds (1.35Å), with a range of 1.30–1.36Å in the literature [20]. For aromatic C–C bonds; for CMT molecule: C1–C16 = 1.413Å, C12–C13 = 1.403Å, C13–C14 = 1.382Å, Typical aromatic C–C bonds are reported as 1.39–1.41Å in the literature. [15, 21, 22]. The bond lengths obtained with Gaussian09 are in good agreement with the structures reported in the literature for both the Thiadiazole–C–S and imidazole–N–C/N–N bonds. Furthermore, the aromatic C–C bond predictions lie within the expected range of 1.39–1.41Å, indicating the reliability of the computational model. In this context, the theoretical geometry of the CMT molecule is consistent and accurate with the existing literature data. Calculated angles for CMT molecule: C1–N5–N4: 108.9° (B3LYP), 108.5° (MPW1PW91), N6–C3–S2: 139.7° (both methods), C8–C7–C9: 130.9°, C20–C19–Cl22: 119.8°. Angles measured in similar rings in the literature: N–C–N angles in imidazo[2,1-

b][1,3,4]thiadiazole derivatives are reported to be between 107–109°. Bond angles around halogenated carbons vary between 118–121° [23, 24]. When the Planar (Torsion) Angles for the CMT molecule are examined (C1–C16–C17–C18 and C13–C12–O15–C23 179.9°), it is seen that the molecule is largely planar. These results are in high agreement with similar imidazo[2,1 b][1,3,4]thiadiazole derivatives in the literature. Anilkumar et al. reported only 5.2(1)° torsion angle between the hetero-ring and the phenyl ring in the crystal structure of 6-(4 chloro phenyl)imidazo[2,1 b][1,3,4]thiadiazole-2-sulfonamide, which reveals that the rings are almost completely coplanar [23]. Hoong KunFun et al. also determined only 5.07(8)° dihedral angle between the plane of imidazo-thiadiazole ring and phenyl ring in the structure of 6-(4 chlorophenyl)-2 isobutylimidazo[2,1-b][1,3,4]thiadiazole, indicating that the structure exhibits high level of conjugation and planarity [25]. These findings support the reliability of the theoretical optimizations performed and the consistency of the molecular geometry with the literature. A similar structure was studied by crystallography for the compound 2-[6-(4-chlorophenyl)imidazo[2,1-b][1,3]thiadiazole]-N′-[(E)-4-methoxybenzylidene]acetohydrazide, and the molecule was reported to have a nearly planar geometry. The study reported that the dihedral angle between the imidazo and thiadiazole rings was only 1.9(2)°, the angle between the heteroaromatic nucleus and the 4-chlorophenyl ring was 5.5(2)°, and the inclination of the methoxyphenyl group with respect to the nucleus was 39.9(2)°. These values are in high agreement with theoretical results calculated for similar structures and support the preservation of molecular planarity [26]. The crystal structure of the structurally similar compound 6(4chlorophenyl)2isobutylimidazo[2,1b][1,3,4]thiadiazole was also investigated, and the imidazo[2,1b][1,3,4]thiadiazole core was determined to be planar. In this study, the chlorophenyl group was reported to be inclined only 5.07(8)° relative to the core plane, i.e., positioned very close to the plane. Furthermore, the bond lengths of S1–C9 and S1–C10 were reported to be 1.772(4) Å and 1.724(2) Å, respectively, and these differences were attributed to resonance effects [27].

Table 1. The CMT molecule's theoretically computed some bond angles (°) and bond lengths (Å)

Bond Lengths	DFT/B3LYP 6-311G(d,p)	DFT/MPW1PW91 6-311G(d,p)	Bond Lengths	DFT/B3LYP 6-311G(d,p)	DFT/MPW1PW91 6-311G(d,p)
C1-C16	1.41344	1.40886	**C1-S2**	1.85994	1.83407
C7-C8	1.37394	1.37039	**C3-S2**	1.72981	1.71799
C9-C10	1.39945	1.39465	**C7-N6**	1.39451	1.38562
C12-C13	1.40260	1.39847	**C1-N5**	1.35476	1.35219
C13-C14	1.38186	1.37802	**C3- N4**	1.34976	1.34250
C16-C17	1.42544	1.42006	**C3-N6**	1.35949	1.35217
C17-C18	1.38049	1.37669	**C12-O15**	1.35740	1.34861
C19-C20	1.39359	1.39060	**N6-H24**	1.00687	1.00462
C20-C21	1.38501	1.38088	**C8-H25**	1.07428	1.07393
C19-CI22	1.76541	1.74607	**C23-H36**	1.09525	1.09458
Bond Angles	**DFT/B3LYP 6-311G(d,p)**	**DFT/MPW1PW91 6-311G(d,p)**	**Bond Angles**	**DFT/B3LYP 6-311G(d,p)**	**DFT/MPW1PW91 6-311G(d,p)**
C1-N5-N4	108.87924	108.46666	**C17-C18-C19**	119.98621	120.06407
C8-C7-C9	130.87539	130.83858	**C16-C21-C20**	121.37844	121.33272
C13-C12-O15	115.79954	115.90622	**C20-C21-H33**	118.41283	118.46211
N6-C3-S2	139.67706	139.69832	**C16-C1-S2**	120.41415	120.26634
C20-C19-CI22	119.79148	119.85349	**C3-N6-H24**	124.96604	125.15470
Planar Bond Angles	**DFT/B3LYP 6-311G(d,p)**	**DFT/MPW1PW91 6-311G(d,p)**	**Planar Bond Angles**	**DFT/B3LYP 6-311G(d,p)**	**DFT/MPW1PW91 6-311G(d,p)**
C1-C16-C17-C18	179.89802	179.92701	**C13-C12-O15-C23**	179.93435	179.95025
C17-C18-C19-CI22	179.94508	179.94966	**C9-C7-N6-C3**	178.52409	178.77696
N5-N4-C3-N6	177.55235	177.97238	**C12-C11-C10-H26**	177.14545	177.11874
C7-N6-C3-S2	178.40718	178.93366	**C13-C12-C11-H27**	179.16927	179.13711

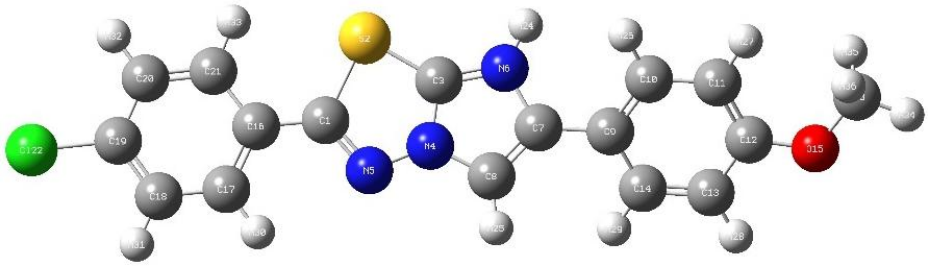

Figure 1. Optimized geometry display of molecule CMT utilizing the B3LYP/6-311G(d,p) method and basis set

B. Mulliken Atomic Charges

One of the most common and traditional techniques for charge analysis is the Mulliken charge distribution. This method is utilized to study the distribution of electrons between molecules and is particularly important in the analysis of chemical bonds [28, 29]. Mulliken charge analysis attempts to determine how the charges on each atom of the molecule are distributed. Mulliken charge calculates how the wave function of the molecule will be distributed in each atomic orbital and determines the sharing of each of these orbitals between atoms [30]. In this way, information is obtained about the total charge of an atom in the molecule. It illustrates how each atom's electron density is positioned. Because the amount of charge on an atom may alter its chemical reactivity, it is utilized to understand the electrical characteristics of molecules [31]. Utilizing the B3LYP, MPW1PW91 methods and the 6-311G(d,p) basis set, the CMT compound's the Mulliken atomic charges were calculated and these calculated values have been given in Table 2. When we compare the Mulliken atomic charges calculated utilizing two different methods, they have values close to each other except for C12 and CI22 atoms. It was discovered that while some C atoms have a positive charge, some have a negative charge. It was observed that the electronegative atoms (N4, N5, N6, O2 and CI22) in the CMT molecule have negative charge values.

Table 2. Mulliken Atomic Charges of the CMT molecule's

ATOMS	DFT/B3LYP 6-311G(d,p)	DFT/MPW1PW91 6-311G(d,p)	ATOMS	DFT/B3LYP 6-311G(d,p)	DFT/MPW1PW91 6-311G(d,p)
C1	-0.035	-0.017	**N6**	-0.418	-0.465
C7	0.102	0.106	**O15**	-0.341	-0.346
C9	-0.086	-0.101	**CI22**	-0.107	-0.196
C10	-0.059	-0.062	**S2**	0.217	0.246
C11	-0.133	-0.147	**H24**	0.252	0.262
C12	0.101	0.192	**H25**	0.129	0.138
C13	-0.088	-0.100	**H26**	0.090	0.100
C14	-0.050	-0.051	**H27**	0.111	0.127
C16	-0.044	-0.068	**H28**	0.112	0.122
C17	-0.044	-0.041	**H29**	0.101	0.110
C18	0.015	0.013	**H30**	0.092	0.101
C19	-0.250	-0.274	**H31**	0.106	0.116
C20	0.012	0.009	**H32**	0.104	0.133
C21	-0.110	-0.121	**H33**	0.084	0.096
N4	-0.192	-0.222	**H34**	0.137	0.147
N5	-0.252	-0.286	**H36**	0.116	0.130

C. Molecular Electrostatic Potential (MEP)

MEP describes the electrical potential at the surface of a molecule and is used to understand how molecules can interact. MEP is shaped by the charge distribution of the atoms of the molecule and shows the potential effects of this distribution on the molecule's the surface [18, 32-34]. The molecule's the electrical potential is related to the bonds between the atoms, electron densities and especially charge separations. MEP is used to predict electrostatic interactions between molecules [35]. It plays a significant role in biological systems, protein-ligand interactions and drug design. MEP defines positive (acceptor) and negative (donor) regions on the surface of a molecule. This provides information about how the molecule can interact with other molecules. In areas with low electron density, the positive electrostatic potential repels the proton, whereas the negative electrostatic potential defines the proton's attraction to the electron density [36]. Chemically active areas of a molecule are linked to MEP, which also enhances perceptions of electrophilic reactions, substituent effects, intermolecular and intramolecular interactions, and molecular reactivity. The electrostatic potential increases in the following order: red, yellow, blue, and green [37]. Using B3LYP, MPW1PW91 methods and 6-311G(d,p) basis set, MEP of CMT compound was calculated and MEP map of the molecule has been given in Figure 2. The highest electrostatic potential or nucleophilicity has been given by the blue region, while the lowest electrostatic potential or electrophilicity has been represented by the red region. When we examine the MEP map in Figure 2, we observed that the blue region is commonly found and the highest electrostatic potential or nucleophilicity. The lone oxygen atom caused the molecule to be somewhat electron rich (yellow) on the color scale, while the hydrogen atoms were in the electron-deficient (blue) area. The electronegative nitrogen atom's bonding with the hydrogen atoms is the cause of this.

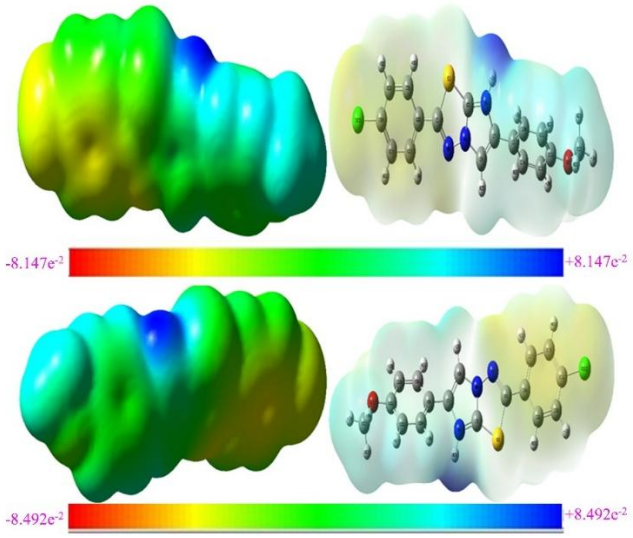

Figure 2. MEP map CMT using B3LYP, MPW1PW91 methods and 6-311G(d,p) basis set

D. HOMO and LUMO Analysis

HOMO and LUMO analyses are concepts utilized to study molecular structures, playing a significant role in understanding physical and chemical properties. This analysis is frequently used, especially in the field of quantum chemistry and molecular modeling [38, 39]. HOMO is especially important in understanding the behavior of molecules that donate electrons. Because electrons in the HOMO of a molecule can be transferred to another molecule (usually an acceptor). This plays a significant role, especially in the initiation of chemical reactions or redox processes. If a molecule has a high energy HOMO, it can more easily donate electrons (be an electron donor) [40]. The LUMO is the lowest energy molecular orbital in a molecule which does not contain electrons. Electrons could fill the vacant positions in this orbital. The LUMO is often used to understand the properties of a molecule that accepts electrons. In chemical reactions, the LUMO of a molecule can be an orbital that can interact with another molecule [41]. The LUMO energy indicates the molecule's the chemical reactivity and how easily it can accept electrons. If the LUMO of a molecule is low in energy, it can more easily accept electrons (be an electron acceptor). We show the HOMO-LUMO energy diagram (Figure 3 and Figure 4) utilizing the B3LYP, MPW1PW91 methods and the 6-311G(d,p) basis set, showing the electron-rich region (red) and the electron-rich region (green). When we examine Figure 3 and Figure 4, we see that the LUMO+1 electron clouds are localized on the imidazo[2,1-b][1,3,4]thiadiazole ring in both methods. While the HOMO-1 was localized on the imidazo[2,1-b][1,3,4]thiadiazole ring in the B3LYP method, it was localized on the benzene ring in the MPW1PW91 method. We observed that in both sets of localized sites HOMO-1 is differently localized and LUMO+1 is the same localized, indicating that the frontier molecular orbitals have important roles in chemical reactivity and stability. Table 3 shows the theoretically calculated electrical structural properties of the CMT molecule. Table 3 shows that the B3LYP method gives HOMO -6.124 eV / LUMO -3.027 eV, and the MPW1PW91 method gives HOMO -6.124 eV / LUMO -3.139 eV. The energy difference between HOMO and LUMO is an important parameter that determines the chemical reactivity of a molecule. This energy difference indicates how easily the molecule can give or take electrons. If the HOMO-LUMO energy difference is small, the molecule is more reactive because electrons can move more easily. If the HOMO-LUMO energy difference is large, the molecule is more stable and less reactive because electrons have difficulty moving. The HOMO-LUMO energy difference calculated by the B3LYP method was found to be 3.097 eV and the MPW1PW91 method was found to be 2.985 eV. Since the energy difference calculated by the MPW1PW91 method is smaller than the energy difference calculated by the B3LYP method, we think that the molecule may be more reactive according to this method.

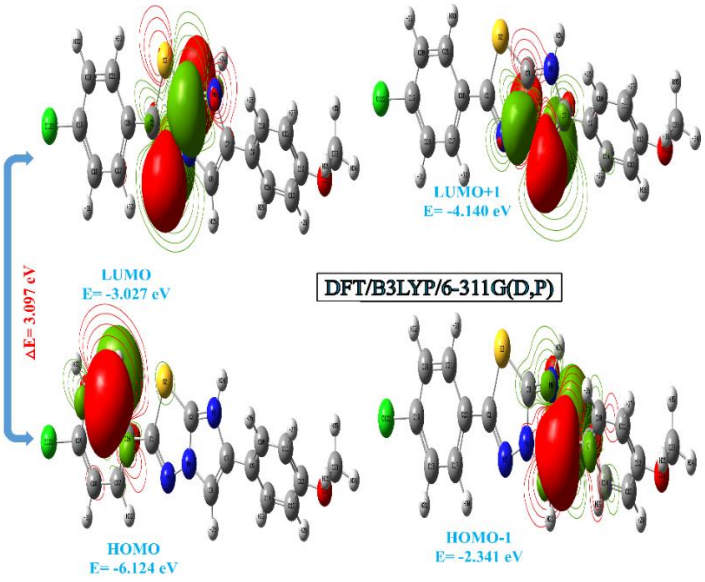

Figure 3. Pictures of molecular frontier orbitals utilizing the B3PW91 method

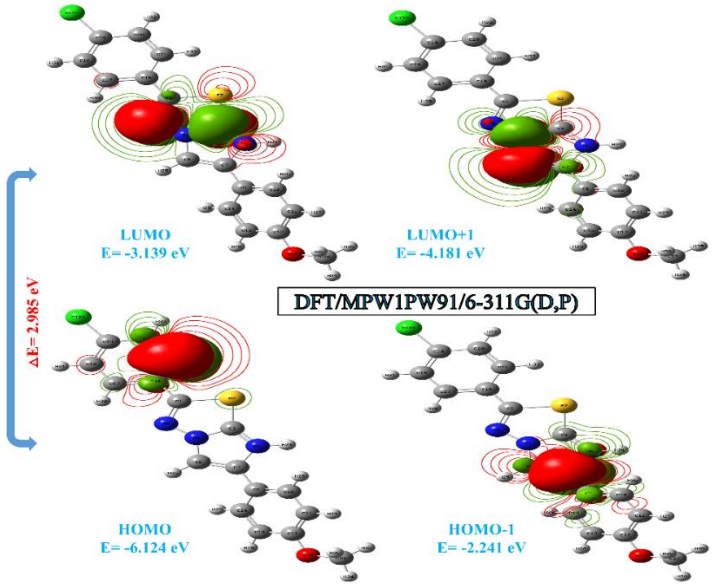

Figure 4. Pictures of molecular frontier orbitals utilizing the B3LYP method

Table 3. The CMT molecule's calculated electrical structural characteristics

Molecules Energy		**B3LYP 6-311G(d,p)**	**MPW1PW91 6-311G(d,p)**
E_{LUMO}		-3.027	-3.139
E_{HOMO}		-6.124	-6.124
E_{LUMO+1}		-4.140	-4.181
E_{HOMO-1}		-2.341	-2.241
Energy Gap	$(\Delta E)\lvert E_{HOMO}-E_{LUMO}\rvert$	3.097	2.985
Ionization Potential	$(I=-E_{HOMO})$	6.124	6.124
Electron Affinity	$(A=-E_{LUMO})$	3.027	3.139
Chemical hardness	$(\eta=(I-A)/2)$	3.097	2.985
Chemical softness	$(s=1/2\eta)$	1.5485	1.4925
Chemical Potential	$(\mu=-(I+A)/2)$	-4.5755	-4.6315
Electronegativity	$(\chi=(1+A)/2)$	2.0135	2.0695
Electrophilicity index	$(\omega=\mu^2/2\eta)$	3.3799	3.5931

E. NBO Analysis

Natural Bonding Orbital (NBO) is a method of analysis of molecular orbitals and is widely used in chemistry, especially in quantum chemistry calculations [42, 43]. NBO is a significant tool to understanding the structural properties of a molecule and the character of its bonds. This concept was developed to explain the bonds within the molecule not only with molecular orbitals but also by determining them in a more natural way. Natural Bonding Orbital (NBO) is a powerful tool which enables the chemical structure of a molecule to be analyzed in a more natural way [44]. It is used based on quantum chemistry calculations to provide information such as electron distribution, bond strengths, and chemical reactivity of the molecule. Natural Bonding Orbital analysis can show energy transitions of acceptors and donors [45]. The study of intramolecular and intermolecular interactions has been promoted by NBO. In NBO analysis, the electron donor (i) (filled) and electron acceptor (j) (empty) bonds have been examined using a second-order Fock matrix. The 6-311G(d,p) basis set for the parent compound and the MPW1PW91 technique have been used for NBO.

The expected stabilization and acceptor-donor orbital energies E(2) for the charge transfer interaction have been displayed in Table 4. The study of intramolecular and intermolecular interactions has been promoted by NBO. In NBO analysis, the electron donor (i) (filled) and electron acceptor (j) (empty) bonds have been examined using a second-order Fock matrix. The 6-311G(d,p) basis set for the parent compound and the MPW1PW91 technique were used for NBO. The expected stabilization and acceptor-donor orbital energies E(2) for the charge transfer interaction have been displayed in Table 4. In the molecule studied, these bonds, along with their transition states and energy values, are as follows: π(C18-C19)→π*(C16-C17) 47.70 kcal/mol, π(C7-C8)→π*(C9-C10) 32.01 kcal/mol, π(C1-N5)→π*(C1-N5) 16.96 kcal/mol and π(C9-C10)→π*(C7-C8) 11.24 kcal/mol.

Table 4. The CMT molecule's selected NBO results computed using B3PW91method

NBO(i)	Type	Occupancies	NBO(j)	Type	Occupancies	E(2)[a] (Kcal/mol)	E (j)-E(i)[b] (a.u.)	F (i, j)[c] (a.u)
C1-N5	σ	0.96763	**C16-C17**	σ*	0.14242	3.53	0.36	0.048
N6- C7	π	0.98547	**S2-C3**	π*	0.01476	4.59	0.94	0.083
C7-C8	σ	0.95765	**C9-C10**	σ*	0.11950	4.49	0.32	0.050
C9-C10	σ	0.89845	**C7-C8**	σ*	0.15419	6.91	0.29	0.058
C9-C10	σ	0.89845	**C11-C12**	σ*	0.12416	4.85	0.30	0.049
C9-C10	σ	0.89845	**C13-C14**	σ*	0.08594	5.29	0.31	0.051
C9-C10	π	0.98971	**C13-C14**	π*	0.00443	3.08	0.93	0.068
C11-C12	σ	0.90246	**C9-C10**	σ*	0.11950	5.68	0.32	0.054
C11-C12	σ	0.90246	**C13-C14**	σ*	0.08594	4.89	0.31	0.050
C13-C14	σ	0.91714	**C9-C10**	σ*	0.11950	5.40	0.31	0.053
C13-C14	σ	0.91714	**C11-C12**	σ*	0.12416	5.65	0.31	0.054
C16-C17	σ	0.88384	**C1-N5**	σ*	0.21398	6.28	0.25	0.053
C16-C17	σ	0.88384	**C18-C19**	σ*	0.14006	6.21	0.29	0.054
C16-C17	σ	0.88384	**C20-C21**	σ*	0.08793	5.14	0.30	0.050
C17-C18	π	0.98166	**C19-Cl22**	π*	0.01599	3.36	0.74	0.063
C17-H30	σ	0.98886	**C16-C21**	σ*	0.01559	3.19	0.92	0.068
C18-C19	σ	0.91082	**C16-C17**	σ*	0.14242	4.44	0.32	0.049
C18-C19	σ	0.91082	**C20-C21**	σ*	0.08793	5.54	0.32	0.053
C20-C21	σ	0.91590	**C16-C17**	σ*	0.14242	5.42	0.31	0.054
C20-C21	σ	0.91590	**C18-C19**	σ*	0.14006	4.89	0.30	0.050
C1-N5	π	0.21398	**C16-C17**	π *	0.14242	16.96	0.06	0.066
C7-C8	π	0.15419	**C9-C10**	π*	0.11950	32.01	0.02	0.060
C18-C19	π	0.14006	**C16-C17**	π*	0.14242	47.70	0.02	0.067
C18-C19	π	0.14006	**C20-C21**	π*	0.08793	53.84	0.01	0.062

F. Non-Linear Optical Properties (NLO)

Quantum chemical computations are used to study the behavior of nonlinear optics. The interplay of electromagnetic fields results in NLO activity. Nonlinear optical activity has applications in bright materials, optical signals, telecommunications, molecular switches, and electrochemical sensors. Due to their extensive application in several scientific domains, NLO materials have garnered more attention recently [46]. Good NLO properties can be found in numerous photonic applications, including digital communication, signal processing, optical computing, sensors and the creation of optical interconnect materials. An isolated molecule has a dipole moment change when an external electric field is present. Therefore, in the equation for the total dipole moment, first and second order contributions appear, as well as the permanent dipole moment [47]. The α-polarizability, μ-electric dipole moment, and β-hyperpolarizability values calculated utilizing B3LYP, MPW1PW91 methods and 6-311G(d,p) basis set for the title compound at various solvations have been shown in Table 5. Equations (1-3) were then used to calculate the average molecular polarizability value in Cartesian coordinates from the output file. The dipole moments of CMT compound calculated by B3LYP and MPW1PW91 methods are 6.2597, 5.9512, and the first order hyperpolarizability is 2.63×10^{-30}, 2.62×10^{-30}, respectively. Urea molecule is one of the model molecules utilized in the studies on systems exhibiting NLO properties. According to the calculations, the μ and β

values for both methods are around four and seven times greater than those of the common NLO material "urea." In polar solvents, the chemical with the title exhibits significant NLO activity. The claim that the title molecule is an active NLO substance is supported by this.

$$\mu = (\mu_x^2 + \mu_z^2)^{1/2} \quad (1)$$

$$\beta_{Total} = (\beta^2 x + \beta^2 y + \beta^2 z)^{1/2} \quad (2)$$

$$= [(\beta xxx + \beta xyy + \beta xzz)^2 + (\beta yyy + \beta yxx + yzz)^2 + (\beta zzz + \beta zxx + \beta zyy)^2]^{\frac{1}{2}} \quad (3)$$

Table 5. The polarizability (au), dipole moments (Debye), components, and total value of molecule CMT computed utilizing B3LYP, MPW1PW91 methods

Parameters	B3LYP 6-311G(d,p)	MPW1PW91 6-311G(d,p)	Parameters	B3LYP 6-311G(d,p)	MPW1PW91 6-311G(d,p)
μ x	5.5721	5.2176	**β XXX**	265.9138	252.7748
μ y	1.8984	1.7802	**β YYY**	-4.2104	-4.7359
μ z	2.1288	2.2423	**β ZZZ**	18.1363	19.4646
μ (D)	6.2597	5.9515	**β XYY**	13.5081	12.5514
α XX	-150.5949	-146.7330	**β XXY**	76.3318	74.3412
α YY	-133.7086	-131.8728	**β XXZ**	92.8499	99.5425
α ZZ	-153.3637	-152.8741	**β XZZ**	34.4034	34.4679
α XY	4.4569	4.6455	**β YZZ**	-2.5995	-2.7669
α XZ	11.5094	11.5571	**β YYZ**	0.6740	0.8114
α YZ	7.5246	8.0849	**β XYZ**	4.9390	5.3433
α (au)	5.9649	5.6790	**β (esu)**	2.63×10^{-30}	2.62×10^{-30}

G. In silico studies

1. ADME Analysis

The drug research and development process relies heavily on the prediction of ADME characteristics to develop effective and safe drugs. ADME provides critical information to understand how a drug acts in the body and what biological effects it produces. Each stage can affect the drug's efficacy, safety and potential side effects. Accurate prediction of ADME data is critical to the drug development process and can affect the clinical success of drugs [48]. The physicochemical properties and drug similarity (Lipinski rules) of the CMT compound were predicted using the SwissADME web (http://swissadme.ch/index.phpundefined). Lipinski rules are a set of chemical rules developed to predict whether a compound is biologically active or not [49]. These rules are used particularly in drug discovery and development processes. Developed by Dr. Christopher A. Lipinski in 1997, Lipinski's rules help predict the bioavailability (i.e., ability to work effectively in the body) of a compound by taking into account certain properties of the molecular structure [50]. The predicted results have been given in Table 6. When we examine the values in Table 6, according to Lipinski's five important rules; having less than 5 hydrogen bond donors (0), less than 10 hydrogen bond acceptors (3), lipophilicity coefficient LogP being less than 5 (4.26), molar refraction values between 4-130 (93.24) and finally We found that the molecular weight (MW) being lower than 500 (341.81) fits. It demonstrates that Lipinski's criteria have not been broken and that this molecule is appropriate for the drug development process. Using %A=109-(0.345xTPYA) to compute the percent absorption, the compounds had a decent absorption profile of 85.65%. The color regions and physicochemical parameters of molecule CMT have been shown in Figure 5. When we examine Figure 5, The pink region on polar surface area maps symbolizes the physicochemical area suitable for oral bioavailability. According to the radar diagram, it is aside from the saturation setting, in the pink region. LogP is a measure of the lipophilicity or hydrophobicity of the compound. A medication is considered lipophilic if its LogP value is more than zero, and hydrophilic if its LogP value is less than zero. The fact that the compound's LogP>0 (4.26) indicates that it is a lipophilic medication. Lipinski's rule states that a good medicine should have a topological polar surface area (TPSA) of less than 140 Å. This is one of the most significant chemical descriptors that corresponds strongly with PK parameters. The TPSA value of HMFC compound was calculated as 85.65 and we think that it will be evaluated as a good drug candidate.

Table 6. Physicochemical and lipophilicity of molecule CMT

Code	Lipophilicity	Physico-chemical properties								
CMT	consensus log P	MW[a] g/mol	Heavy Atoms	Aromatic heavy atoms	Rot. bond	H-acceptor bond	H-donor bond	MR[b]	TPSA[c] (A^2)	% ABS[d]
	4.26	341.81	23	20	3	3	0	93.24	67.66	85.65

[a]**MW**, molecular weight; [c]**TPSA**, topological polar surface area; [b]**MR**, molar refractivity; [d]**ABS%:** absorption percent $ABS\% = 109 - [0.345 \times TPSA]$.

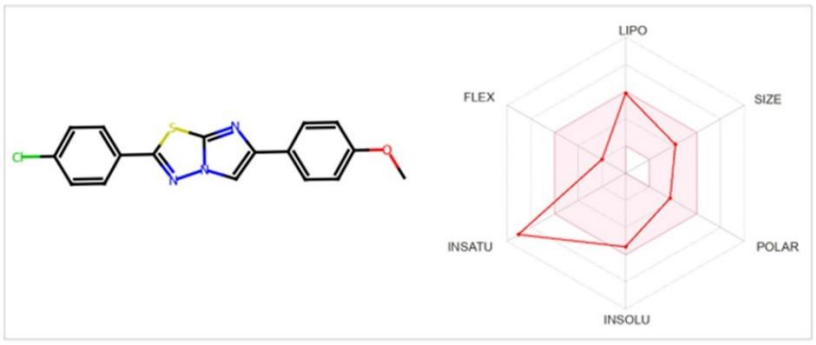

Figure 5. Color regions and physicochemical parameters of molecule CMT

2. Molecular docking studies

The preferred orientation of a molecule (usually a medication or ligand) when attached to another molecule (usually a receptor or protein) may be predicted computationally using a technique called molecular docking. Molecular docking studies' purpose is to understand how two molecules interact, discover possible binding sites, and evaluate the strength of their interactions [51]. This is an important step in drug design, where researchers use docking simulations to forecast how a new drug might interact with its desired protein [52]. Molecular docking analysis was performed with Maestro 11.8 software [13]. The protein crystal structure (3PP0 and 1M17) of the compound was selected using the Protein Data Bank [12]. Utilizing the protein preparation wizard, the protein was created by adding hydrogen atoms and removing water molecules. Clicking on any ligand atom launched the Receptor Grid Creation application and created the default grid box. Using Standard Precision, the ligand was attached to the protein grid box (SP). In the study, the potential of CMT compound on breast cancer was calculated in silico by molecular docking analysis. According to the docking analysis outcomes, CMT compound's the docking score was calculated as -10.20 and -7.50 kcal/mol, respectively, and has been given in Table 7. The docking analysis showed that the theoretical data on breast cancer correlated well with the observed values. Considering the high binding affinity of CMT compound, we believe that the chemical we examined will be an important drug candidate in the creation of structure-based drugs for breast cancer. It was also shown that CMT compound 3PP0 enzyme has a higher docking score than 1M17 enzyme and has the ability to inhibit the biological process of the protein at a higher rate. Using Discovery Studio Client 2017 program, good docking positions were selected for docking analysis and protein-ligand interaction and molecular docking images have been given in Figure 7 and Figure 9. The significant interactions, amino acids and bond lengths of the CMT compound in the docking analysis have been given in Tables 8 and 9. The bond lengths calculated for the CMT molecule are consistent with experimental and theoretical data obtained with similar structures in the literature, supporting a reliable prediction of the molecule's potential biological activity. In particular, the C–S, C–N, and C–O bond lengths, which contain electrophilic and nucleophilic centers and heterocyclic systems (imidazo[2,1b][1,3,4]thiadiazole nuclei), which can be considered pharmacophore regions, are consistent with the literature. This compatibility allows for the creation of accurate bond structures and interaction surfaces during the molecular docking of ligand-target interactions. Therefore, the agreement of theoretically obtained bond lengths with the literature is a critical parameter that directly affects the validity of interaction models of the molecule with biological targets.

Table 7. Docking score of molecule CMT PDB: 3PP0 and PDB: 1M17

Compound	**Docking Score**			
	(PDB: 3PP0)	Control Ligand	(PDB:1M17)	Control Ligand
CMT	-10.20	-10.90	-7.50	-8.30

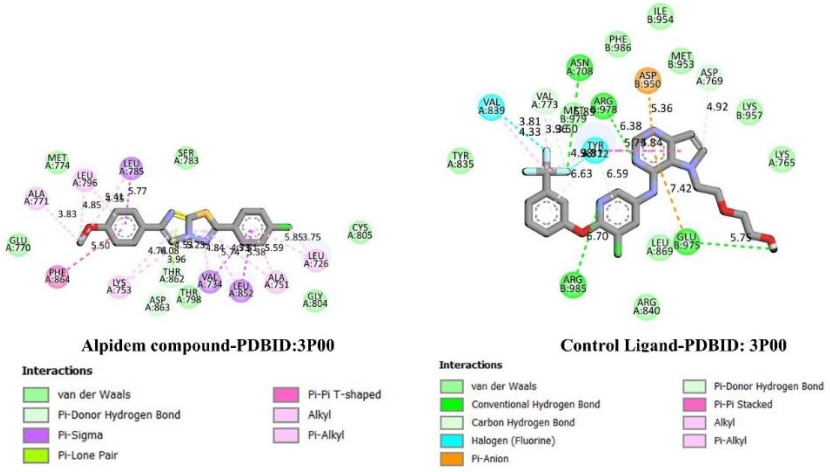

Figure 6. 2D Mode view of CMT Compound-PDBID: 3P00 and control ligand-PDBID: 3P00

Table 7 shows the docking scores obtained in the molecular docking analysis of the CMT compound (calculated docking score -10.20) and the control ligand (2-{2-[4-({5-chloro-6-[3-(trifluoromethyl)phenoxy]pyridin-3-yamino)-5H-pyrrolo[3,2-d]pyrimidin-5-yl]ethoxy}ethanol) (calculated docking score -10.90) with the 3PP0 protein. When we look at the docking scores in Table 7, it is seen that the binding scores for the CMT compound are close to the binding scores of the natural ligand. Figure 6 shows the 2D mode image of the Alpidem compound and the control ligand with 3PP0 protein. When we examine Figure 6, we observe that the targets in question carry different amino acids other than the amino acids found in the receptor binding sites and the compound classes that interact with the targets, namely Van der Waals, Pi-Donor Hyrogen Bond, Pi-Pi T-shaped, Pi-Alkyl.

Table 8. Parameters of the interaction between CMT compound of 3PP0 enzym

Important Interactions	Full Name	Type	Bond Length (Å)	Color
Van der Waals	GLU770	GlutamicAcid	-	
	MET774	Methionine	-	
	SER783	Serine	-	
	CYS805	Cysteine	-	
	ASP863	AsparticAcid	-	
Pi Donor Hydrogen Bond	THR862	Threonine	3.23	
	ASP863	AsparticAcid	3.96	
Pi-Sigma	LEU785	Leucine	5.77	
	VAL734	Valine	5.74	
	LEU852	Leucine	5.38	
Pi-Lone Pair	THR862	Methionine	4.53	
Pİ-Pi T-Shaped	PHE864	Phenylalanine	5.50	
Alkyl	ALA771	Alanine	3.83	
	LEU796	Leucine	4.85	
Pi-Alkyl	LYS753	Lysine	4.76	
	VAL734	Valine	4.84	
	LEU726	Leucine	5.59	
	ALA751	Alanine	5.85	

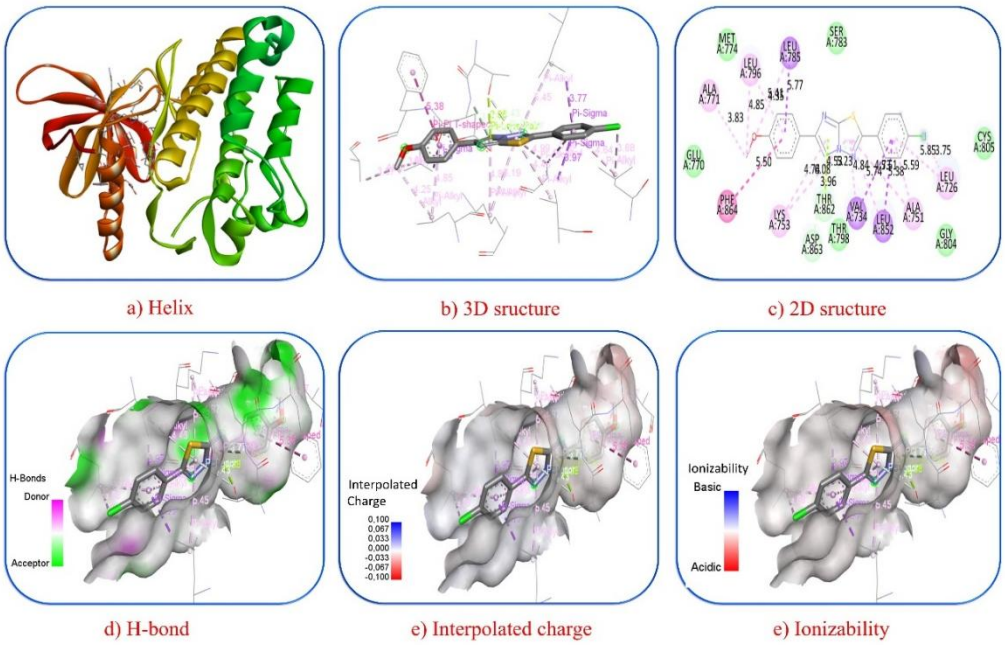

Figure 7. Molecular docking visual results of CMT compound with 3PP0 enzyme

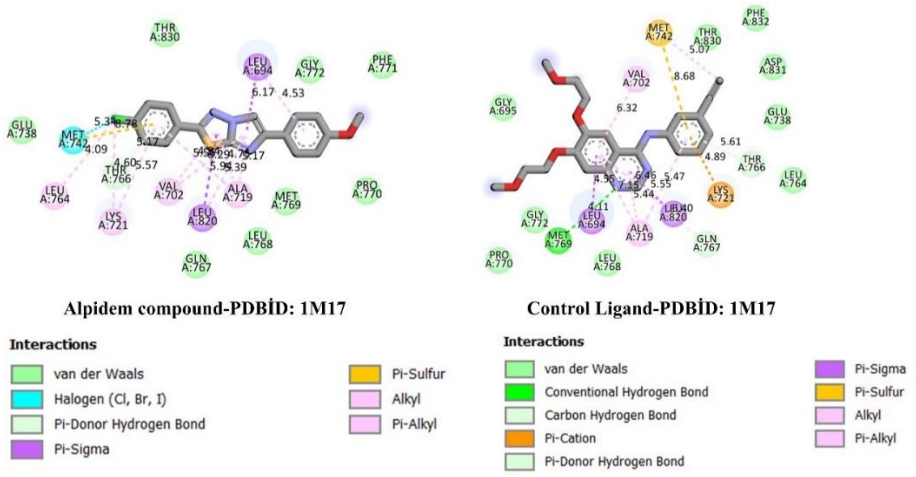

Figure 8. 2D Mode view of CMT Compound-PDBID: 1M17 and control ligand-PDBID: 1M17.

Table 7 presents the docking scores obtained in the molecular docking analysis of the CMT compound (calculated docking score -7.50) and the control ligand [6,7-bıs(2-methoxy-ethoxy)quınazolıne-4-yl]-(3-ethynylphenyl)amıne (calculated docking score -8.30) with the 1M17 protein. When we look at the docking scores in Table 7, it is seen that the binding scores for the CMT compound are close to the binding scores of the natural ligand. Figure 8 shows the 2D mode image of the Alpidem compound and the control ligand with the 1M17 protein. When we examine Figure 8, we observed that the targets in question carry different amino acids other than the amino acids found in the receptor binding sites and the compound classes that interact with the targets, namely Pi-Donor Hyrogen Bond, Van der Waals, Pi-Sigma, Alkyl, PI-Sulfur, Pi-Alkyl.

Table 9. Parameters of the interaction between CMT compound of 1M17 enzym

Important Interactions	Full Name	Type	Bond Length (Å)	Color
Van der Waals	GLU738	GlutamicAcid	-	
	THR830	Threonine	-	
	GLY772	Glycine	-	
	PHE771	Phenylalanine	-	
	MET769	Methionine	-	
Halogen (Cl,Br, I)	MET742	Methionine	5.34	

Pi Donor Hydrogen Bond	THR766	Threonine	4.60	
Pi-Sigma	LEU820 LEU694	Leucine Leucine	5.94 5.74	
Pİ-Sulfur	MET742	Methionine	8.78	
Alkyl	LEU764 LYS721	Leucine Lysine	4.09 5.57	
Pi-Alkyl	LYS721 ALA719 VAL702	Lysine Valine Valine	4.76 4.84 4.59	

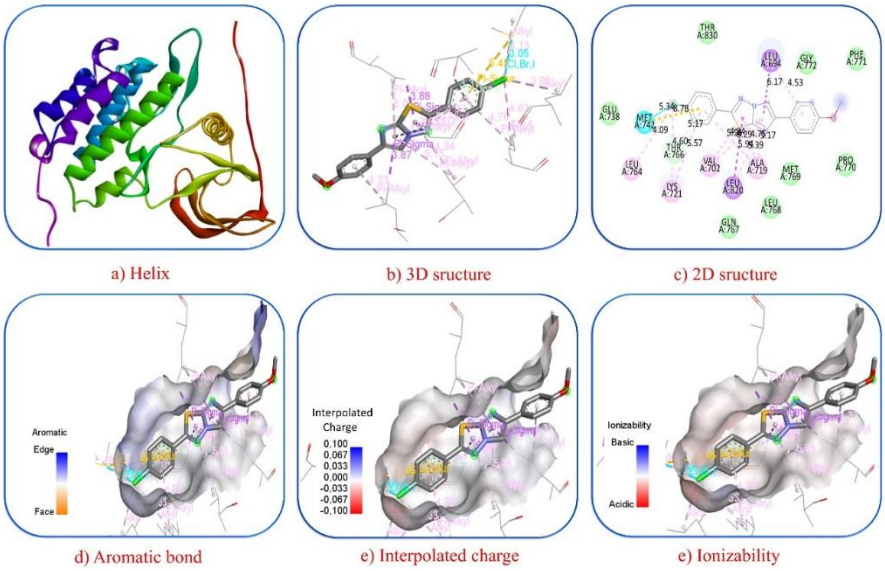

Figure 9. Molecular docking visual results of CMT compound with 1M17 enzyme

IV. CONCLUSION

The first step in our research was to optimize the geometry to discover the lowest energy or stable structure of the molecule with two different methods. During the optimization process, the molecule's the bond lengths and bond angles were determined with two different methods and compared with each other, and it was shown that the molecule's the bond lengths and bond angles were compatible with each other. Then, the total energies and leading molecular orbital energies of the molecule were calculated with two different methods. These energies were shown to agree with each other when compared by calculating the molecular properties (η or electronegativity and η or molecular hardness) based on the HOMOLUMO energy differences in the two different methods. By examining the variations in NBO hybridization % and Mulliken and NBO atomic charge values, it was discovered that there was relatively little variation. In order to provide more information about the molecule under study, MEP energy surface map and NLO characteristics (polarizability, anisotropic polarizability and high polarizability) were determined. In the study, CMT compound was evaluated according to Lipinski rules by performing ADME analysis to evaluate it as a drug. We believe that the analysis outcomes carry Lipinski rules and will be evaluated as a drug. According to ADME research, it has an excellent absorption profile of 85.65% and the findings of the research in the field that produces safe and effective drugs can be used. In the study, 3PP0 and 1M17 enzymes were downloaded from PDB (Protein Data Bank) and the potential of CMT compound on breast cancer was calculated in silico by molecular docking analysis. In the molecular docking study, it was discovered that the optimum docking modes for PDB: 3PP0 and PDB: 1M17 proteins had binding affinities of -10.20 and -7.50 kcal/mol, respectively. The obtained docking scores were good values close to the reference ligand doing scores. We think that this molecular structure can be used to develop new enzyme inhibitors and novel medications to treat breast cancer.

REFERENCES

[1] Bhongade, B.A., Talath, S., Gadad, R.A., Gadad, A.K. (2016). Biological activities of imidazo[2,1-b][1,3,4]thiadiazole derivatives: A review. *Journal of Saudi Chemical Society,* 20, 463-475.

[2] Patel, H.M., Noolvi, M.N., Sethi, N.S., Gadad, A.K., Cameotra, S.S. (2017). Synthesis and antitubercular evaluation of imidazo[2,1-b][1,3,4]thiadiazole derivatives. *Arabian Journal of Chemistry,* 10, 996-1002.

[3] Cristina, A., Leonte, D., Vlase, L., Bencze, L.C., Imre, S., Marc, G., Apan, B., Mogoșan, C., Zaharia, V. (2018). Heterocycles 48. Synthesis, Characterization and Biological Evaluation of Imidazo[2,1-b][1,3,4]Thiadiazole Derivatives as Anti-Inflammatory Agents. *Molecules,* 23(10), 2425.

[4] Lamani, R.S., Shetty, N.S., Kamble, R.R., Khazi, I.A.M. (2009). Synthesis and antimicrobial studies of novel methylene bridged benzisoxazolyl imidazo[2,1-b][1,3,4]thiadiazole derivatives. *European Journal of Medicinal Chemistry,* 44(7), 2828-2833.

[5] Manathunga, M., Götz, A.W., Merz, K.M. (2022). Computer-aided drug design, quantum-mechanical methods for biological problems. *Current Opinion in Structural Biology,* 75, 102417.

[6] Bourass, M., Benjelloun, A.T., Benzakour, M., McHarfi, M., Hamidi, M., Bouzzine, S.M., Bouachrine, M. (2016). DFT and TD-DFT calculation of new thienopyrazine-based small molecules for organic solar cells. *Chemistry Central Journal,* 10(1), 67.

[7] Morgante, P., Peverati, R. (2020). The devil in the details: A tutorial review on some undervalued aspects of density functional theory calculations. *International Journal of Quantum Chemistry,* 120(18), e26332.

[8] Brinkley, D., Haybittle, J.L. (1975). The Curabılıty of Breast Cancer. *The Lancet,* 306(7925), 95-97.

[9] Sun, Y.S., Zhao, Z., Yang, Z.N., Xu, F., Lu, H.J., Zhu, Z.Y., Shi, W., Jiang, J., Yao, P.P., Zhu, H.P. (2017). Risk Factors and Preventions of Breast Cancer. *Int J Biol Sci,* 13(11), 1387-1397.

[10] Ramareddy, A., Karki, S.S. (2012). Sharad Dhepe, Sujeet Kumar, R. Vinayakumar, Sureshbabu. *Med Chem Res,* 21, 1550-1556.

[11] M.J. Frisch, G.W.T., H.B. Schlegel, G.E. Scuseria, M.A. Robb, J.R. Cheeseman, G. Scalmani, V. Barone, B. Mennucci, G.A. Petersson, H. Nakatsuji, M. Caricato, X. Li, H.P. Hratchian, A.F. Izmaylov, J. Bloino, G. Zheng, J.L. Sonnenberg, M. Hada, M. Ehara, K. Toyota, R. Fukuda, J. Hasegawa, M. Ishida, T. Nakajima, Y. Honda, O. Kitao, H. Nakai, T. Vreven, J.A. Montgomery Jr., J.E. Peralta, F. Ogliaro, M. Bearpark, J.J. Heyd, E. Brothers, K.N. Kudin, V.N. Staroverov, R. Kobayashi, J. Normand, K. Raghavachari, A. Rendell, J.C. Burant, S.S. Iyengar, J. Tomasi, M. Cossi, N. Rega, J.M. Millam, M. Klene, J.E. Knox, J.B. Cross, V. Bakken, C. Adamo, J. Jaramillo, R. Gomperts, R.E. Stratmann, O. Yazyev, A.J. Austin, R. Cammi, C. Pomelli, J.W. Ochterski, R.L. Martin, K. Morokuma, V.G. Zakrzewski, G.A. Voth, P. Salvador, J.J. Dannenberg, S. Dapprich, A.D. Daniels, Ö. Farkas, J.B. Foresman, J.V. Ortiz, J. Cioslowski, D.J. Fox, *Gaussian 09*. 2009.

[12] Burley, S.K., Berman, H.M., Bhikadiya, C., Bi, C., Chen, L., Di Costanzo, L., Christie, C., Dalenberg, K., Duarte, J.M., Dutta, S., Feng, Z., Ghosh, S., Goodsell, D.S., Green, R.K., Guranović, V., Guzenko, D., Hudson, B.P., Kalro, T., Liang, Y., Lowe, R., Namkoong, H., Peisach, E., Periskova, I., Prlić, A., Randle, C., Rose, A., Rose, P., Sala, R., Sekharan, M., Shao, C., Tan, L., Tao, Y.-P., Valasatava, Y., Voigt, M., Westbrook, J., Woo, J., Yang, H., Young, J., Zhuravleva, M., Zardecki, C. (2018). RCSB Protein Data Bank: biological macromolecular structures enabling research and education in fundamental biology, biomedicine, biotechnology and energy. *Nucleic Acids Research,* 47(D1), D464-D474.

[13] Release, S., *1: Maestro, Schrodinger, LLC, New York*. 2019.

[14] Studio, B.D. (2016). Dassault Systèmes Biovia Corporation. *San Diego, USA,*

[15] Tahiroğlu, V., Gören, K., Yıldıko, Ü., Bağlan, M. (2024). IInvestigation, Structural Characterization and Evaluation of the Biological Potency by Molecular Docking of Amoxicillin Analogue of a Schiff Base Molecule. *International Journal of Chemistry and Technology,* 8(2), 190-199.

[16] Gören, K., Bağlan, M., Tahiroğlu, V., Yıldıko, Ü. (2024). Theoretical Calculations and Molecular Docking Analysis of 4-(2-(4-Bromophenyl)Hydrazineylidene)-3,5-Diphenyl-4H-Pyrazole Molecule. *Journal of Advanced Research in Natural and Applied Sciences,* 10(4), 786-802.

[17] Uysal, Ü.D. (2012). A DFT Study of Biogenic Amines. *Afyon Kocatepe Üniversitesi Fen Ve Mühendislik Bilimleri Dergisi,* 12(1), 11-24.

[18] Gören, K., Yıldıko, Ü. (2024). Aldose Reductase Evaluation against Diabetic Complications Using ADME and Molecular Docking Studies and DFT Calculations of Spiroindoline Derivative Molecule. *Süleyman Demirel Üniversitesi Fen Bilimleri Enstitüsü Dergisi,* 28(2), 281-292.

[19] Banu, A., Begum, N.S., Lamani, R.S., Khazi, I. (2011). 6-(4-Bromophenyl)-2-(4-fluorobenzyl) imidazo [2, 1-b][1, 3, 4] thiadiazole. *Structure Reports,* 67(4), o779-o779.

[20] Heidarizadeh, F., Saadati, S., Rostami, E. (2024). Evaluation of 1, 3, 4-Thiadiazole and 1, 3-Thiazolidine-4-One Binary Molecules against the SARS-CoV-2 Receptor: DFT Study, PASS Prediction, ADMET Analysis, Molecular Docking, and ADMET Optimization. *Materials Chemistry,* 3, 1067.

[21] Çimen, E., Gören, K., Tahiroğlu, V., Yıldıko, Ü. (2025). The Theoretical Calculations by DFT Method and Analysis ADME, Molecular Docking of 1-(1-(4-hydroxybutyl)-6-methyl-4-phenyl-2-

thioxohexahydropyrimidin-5-yl)ethan-1-one (pyrimidine-thiones) Compound. *Osmaniye Korkut Ata Üniversitesi Fen Bilimleri Enstitüsü Dergisi,* 8(3), 1129-1145.

[22] Gören, K., Bağlan, M., Yıldıko, Ü. (2025). Analysis By DFT, ADME and Docking Studies Of N'-(4-Hydroxy-3-Methoxybenzylidene)Naphtho[2,3-B]Furan-2-Carbohydrazide. *Eskişehir Teknik Üniversitesi Bilim ve Teknoloji Dergisi B - Teorik Bilimler,* 13(1), 7-23.

[23] Efimov, V.V., Krasnov, P.O., Lyubyashkin, A.V., Suboch, G.A., Tovbis, M.S. (2018). Experimental and theoretical study of the acylation reaction of aminopyrazoles with aryl and methoxymethyl substituents. *Journal of Molecular Structure,* 1165, 370-375.

[24] Shamanth, S., Mantelingu, K., Kiran Kumar, H., Yathirajan, H.S., Foro, S., Glidewell, C. (2020). Crystal structures of three 6-aryl-2-(4-chlorobenzyl)-5-[(1H-indol-3-yl)methyl]imidazo[2,1-b][1,3,4]thiadiazoles. *Acta Crystallographica Section E,* 76(1), 18-24.

[25] Fun, H.-K., Hemamalini, M., Prasad, D.J., Nagaraja, G., Anitha, V. (2011). 6-(4-Chlorophenyl)-2-isobutylimidazo [2, 1-b][1, 3, 4] thiadiazole. *Structure Reports,* 67(1), o207-o207.

[26] Akkurt, M., Güzeldemirci, N.U., Karaman, B., Büyükgüngör, O. (2010). 2-[6-(4-Chloro-phen-yl)imidazo[2,1-b][1,3]thia-zol-2-yl]-N'-[(E)-4-meth-oxy-benzyl-idene]acetohydrazide. *Acta Crystallogr Sect E Struct Rep Online,* 67(Pt 1), o184-5.

[27] Banu, A., Ziaulla, M., Begum, N.S., Lamani, R.S., Khazi, I.M. (2011). 3-{[6-(4-Chloro-phen-yl)imidazo[2,1-b][1,3,4]thia-diazol-2-yl]meth-yl}-1,2-benzoxazole. *Acta Crystallogr Sect E Struct Rep Online,* 67(Pt 3), o617-8.

[28] Gören, K., Bağlan, M., Yıldıko, Ü. (2024). Antimicrobial, and Antitubercular Evaluation with ADME and Molecular Docking Studies and DFT Calculatıons of (Z)-3-((1-(5-amino-1,3,4-thiadiazol-2-yl)-2-Phenylethyl)imino)-5-nitroindolin-2-one Schiff Base. *Karadeniz Fen Bilimleri Dergisi,* 14(4), 1694-1708.

[29] Tahiroğlu, V., Gören, K., Çimen, E., Yıldıko, Ü. (2024). Moleculer Docking and Theoretical Analysis of the (E)-5-((Z)-4-methylbenzylidene)-2-(((E)-4-methylbenzylidene)hydrazineylidene)-3-phenylthiazolidin-4-one Molecule. *Bitlis Eren Üniversitesi Fen Bilimleri Dergisi,* 13(3), 659-672.

[30] Govindasamy, P., Gunasekaran, S., Srinivasan, S. (2014). Molecular geometry, conformational, vibrational spectroscopic, molecular orbital and Mulliken charge analysis of 2-acetoxybenzoic acid. *Spectrochimica Acta Part A: Molecular and Biomolecular Spectroscopy,* 130, 329-336.

[31] Senthilkumar †, L., Kolandaivel *, P. (2005). Study of effective hardness and condensed Fukui functions using AIM, ab initio, and DFT methods. *Molecular Physics,* 103(4), 547-556.

[32] Gören, K., Bağlan, M., Yıldıko, Ü. (2024). Melanoma Cancer Evaluation with ADME and Molecular Docking Analysis, DFT Calculations of (E)-methyl 3-(1-(4-methoxybenzyl)-2,3-dioxoindolin-5-yl)-acrylate Molecule. *Journal of the Institute of Science and Technology,* 14(3), 1186-1199.

[33] Tahiroğlu, V., Gören, K., Bağlan, M., Yıldıko, Ü. (2024). Molecular Docking and DFT Analysis of Thiazolidinone-Bis Schiff Base for anti-Cancer and anti-Urease Activity. *Journal of the Institute of Science and Technology,* 14(2), 822-834.

[34] Bağlan, M., Gören, K., Yıldıko, Ü. (2023). HOMO–LUMO, NBO, NLO, MEP analysis and molecular docking using DFT calculations in DFPA molecule. *International Journal of Chemistry and Technology,* 7(1), 38-47.

[35] Lakshminarayanan, S., Jeyasingh, V., Murugesan, K., Selvapalam, N., Dass, G. (2021). Molecular electrostatic potential (MEP) surface analysis of chemo sensors: An extra supporting hand for strength, selectivity & non-traditional interactions. *Journal of Photochemistry and Photobiology,* 6, 100022.

[36] Guin, M., Halder, S., Chatterjee, S., Konar, S. (2022). Synthesis, X-ray crystal structure of Cu(II) 1D coordination Polymer: In View of Hirshfeld surface, FMO, Molecular electrostatic potential (MEP) and Natural Bond orbital (NBO) analyses. *Journal of Molecular Structure,* 1270, 133949.

[37] Silvarajoo, S., Osman, U.M., Kamarudin, K.H., Razali, M.H., Yusoff, H.M., Bhat, I.U.H., Rozaini, M.Z.H., Juahir, Y. (2020). Dataset of theoretical Molecular Electrostatic Potential (MEP), Highest Occupied Molecular Orbital-Lowest Unoccupied Molecular Orbital (HOMO-LUMO) band gap and experimental cole-cole plot of 4-(ortho-, meta- and para-fluorophenyl)thiosemicarbazide isomers. *Data in Brief,* 32, 106299.

[38] Bağlan, M., Gören, K., Yıldıko, Ü. (2023). DFT Computations and Molecular Docking Studies of 3-(6-(3-aminophenyl)thiazolo[1,2,4]triazol-2-yl)-2H-chromen-2-one(ATTC) Molecule. *Hittite Journal of Science and Engineering,* 10(1), 11-19.

[39] Bağlan, M., Yıldıko, Ü., Gören, K. (2023). DFT Calculations and Molecular Docking Study in 6-(2”-pyrrolıdınone-5”-yl)-(-) Epicatechin Molecule from Flavonoids. *Eskişehir Teknik Üniversitesi Bilim ve Teknoloji Dergisi B - Teorik Bilimler,* 11(1), 43-55.

[40] Suhasini, M., Sailatha, E., Gunasekaran, S., Ramkumaar, G.R. (2015). Vibrational and electronic investigations, thermodynamic parameters, HOMO and LUMO analysis on Lornoxicam by density functional theory. *Journal of Molecular Structure,* 1100, 116-128.

[41] Demir, P., Akman, F. (2017). Molecular structure, spectroscopic characterization, HOMO and LUMO analysis of PU and PCL grafted onto PEMA-co-PHEMA with DFT quantum chemical calculations. *Journal of Molecular Structure,* 1134, 404-415.
[42] Bağlan, M., Yıldıko, Ü., Gören, K. (2022). Computational Investigation of 5.5",7"-trihydroxy-3,7-dimethoxy-4'-4"'-O-biflavone from Flavonoids Using DFT Calculations and Molecular Docking. *Adıyaman University Journal of Science,* 12(2), 283-298.
[43] Bağlan, M., Gören, K., Çakmak, İ. (2022). Theoretical Investigation of 1H and 13C NMR Spectra of Diethanol Amine Dithiocarbamate RAFT Agent. *Journal of the Institute of Science and Technology,* 12(3), 1677-1689.
[44] Thakur, T.S., Desiraju, G.R. (2007). Theoretical investigation of C–H···M interactions in organometallic complexes: A natural bond orbital (NBO) study. *Journal of Molecular Structure: THEOCHEM,* 810(1), 143-154.
[45] Halim, S.A., El-Meligy, A.B., El-Nahas, A.M., El-Demerdash, S.H. (2024). DFT study, and natural bond orbital (NBO) population analysis of 2-(2-Hydroxyphenyl)-1-azaazulene tautomers and their mercapto analouges. *Scientific Reports,* 14(1), 219.
[46] Shokr, E.K., Kamel, M.S., Abdel-Ghany, H., El- Remaily, M.A.E.A.A.A., Abdou, A. (2022). Synthesis, characterization, and DFT study of linear and non-linear optical properties of some novel thieno[2,3-b]thiophene azo dye derivatives. *Materials Chemistry and Physics,* 290, 126646.
[47] Abdel Aziz, A.A., Elantabli, F.M., Moustafa, H., El-Medani, S.M. (2017). Spectroscopic, DNA binding ability, biological activity, DFT calculations and non linear optical properties (NLO) of novel Co(II), Cu(II), Zn(II), Cd(II) and Hg(II) complexes with ONS Schiff base. *Journal of Molecular Structure,* 1141, 563-576.
[48] Aycan, T., Öztürk, S., Demircioğlu, Z., Ersanlı, C.C. (2023). Quantum Mechanical Calculations, Hirshfeld Surface Analysis, Molecular Docking, ADME and Toxicology Studies of the Ethyl 4-chloro-2-[(4-nitrophenyl)hydrazono]-3-oxobutrate Compound. *International Scientific and Vocational Studies Journal,* 7(2), 109-121.
[49] Erol, M., Çelik, İ., Kuyucuklu, G. (2021). 2-(p-Florofenil)-5-(2-(4-asetilpiperazin-1-il)asetamido)benzoksazol'ün Sentezi, Moleküler Doking, DFT ve Antimikrobiyal Aktivite Çalışmaları. *Journal of the Institute of Science and Technology,* 11(3), 2122-2132.
[50] Erol, M., Çelik, İ., Kuyucuklu, G. (2021). Bazı Yeni 2,5-Disübstitüe Benzoksazol Türevlerinin Sentezi, Antimikrobiyal Aktivite, Moleküler Doking ve DFT Çalışmaları. *Avrupa Bilim ve Teknoloji Dergisi,* 27), 605-614.
[51] Noureddine, O., Gatfaoui, S., Brandan, S.A., Sagaama, A., Marouani, H., Issaoui, N. (2020). Experimental and DFT studies on the molecular structure, spectroscopic properties, and molecular docking of 4-phenylpiperazine-1-ium dihydrogen phosphate. *Journal of Molecular Structure,* 1207, 127762.
[52] Dlala, N.A., Bouazizi, Y., Ghalla, H., Hamdi, N. (2021). DFT Calculations and Molecular Docking Studies on a Chromene Derivative. *Journal of Chemistry,* 2021(1), 6674261.